# Performance evaluation and characterization of different photovoltaic technologies under the coastal, desertic climate conditions of Lima, Peru

**Luis A. Conde[1], Jesús Montes-Romero[2], Alejandro Carhuavilca[1], Renzo Perich[1], Jorge A. Guerra[1], José Angulo[1], Emilio Muñoz[2], Jan A. Töfflinger[1]* and Juan de la Casa[2]**

[1] Departamento de Ciencias, Sección de Física, Pontificia Universidad Católica del Perú, Av. Universitaria 1801, Lima 32, Perú

*Correspondence author: japalominot@pucp.edu.pe

[2] IDEA Research Group (Research and Development in Solar Energy), Centre for Advanced Studies in Energy and Environment (CEAEMA), Electronics and Automation Engineering Department, University of Jaén, Spain

**Abstract**

This work presents the firsts results of the experimental characterization campaign under outdoor conditions carried out with three different photovoltaic (PV) module technologies: Standard poly-crystalline silicon (poly-Si) aluminum back surface field (Al-BSF) cells, mono-crystalline (c-Si) Heterojunction with Intrinsic Thin-Layer (HIT) cells, and amorphous and microcrystalline silicon (a-Si/µc-Si) thin-film tandem cells. We studied the behavior of these PV technologies and their performance in Lima's desertic and coastal climate during the period from May 2019 to July 2019. For this study, a new outdoor-PV laboratory was implemented at the Pontificia Universidad Católica del Perú (PUCP) with the help of the IDEA research group of the University of Jaén (UJA), Spain. The laboratory enables the characterization of PV modules by extracting the electrical parameters from the current-voltage (*I-V*) curve under outdoor conditions and by measuring the irradiance, the spectral distribution, the panel temperature, and the weather conditions. As a first step, the nominal maximum power of the PV modules under standard test conditions is obtained from the outdoor data. Then, an analysis of the different PV technologies' performance under the local climate conditions is presented by applying the Osterwald and the constant fill factor methods to compare the modeled and experimental maximum power.

*Keywords: Photovoltaic modules, PV technologies, I-V curve, Osterwald, Peru, Lima*

## 1. Introduction

The Peruvian government is currently working on a regulatory framework to encourage investments in renewable energy, to reach 15% of the energy matrix from non-conventional renewable sources by 2030 [1]. There are also rural electrification projects promoted by the Ministry of Energy and Mines (MINEM) for communities that do not have access to the electricity grid (due to the rugged relief of the Andes), and currently one of these projects has 200 thousand PV panels installed for essential electricity services in homes, medical centers and schools [2].

PV modules are commonly cataloged concerning their maximum power generated under specific conditions called Standard Test Conditions (STC) which are: a normal irradiance of 1000 W/m$^2$, a spectral distribution of AM 1.5 and a cell temperature of 25 °C. Because these conditions hardly represent real outdoor operating conditions, an extensive PV characterization campaign is required to know the real performance under the climatic conditions of the installation place. A recent publication (Romero-Fiances et al., 2018), presented a first analysis of the grid-connected PV system performance for two different commercial PV technologies, Al-BSF and a-Si/µc-Si, installed in Lima. However, more detailed studies are needed to understand these PV technologies' behavior on a fundamental basis, and more different technologies need to be compared. This work aims towards achieving a better understanding of the PV performance on module level for different technologies in Lima.

Lima is located on the central west coast of Peru (12° 2'S, 77° 1'W) and, as Peru's capital, is one of the most populated cities in Latin America. Lima has an "arid hot desert climate" as classified in (Kottek et al., 2006) and


doi:10.18086/swc.2019.16.01 Available at http://proceedings.ises.org

has a population of over 10 million [3] that represents one-third of the population of Peru. That is why it is important to study the real behavior of commercial PV technologies and their performance under the local conditions. This information will support Peru's transition towards an electricity supply with more renewable energies to meet the goal of the energy reform that the country has planned [4].

To know the real behavior of PV modules of different technologies, an outdoor module characterization system was implemented with the help of the IDEA research group of the University of Jaen (UJA) in the roof of the Physics section of the Pontificia Universidad Católica del Perú (PUCP). It is the first fully equipped photovoltaic panel characterization laboratory in Peru for research purposes as well as offering PV module evaluation services in the near future.

For the characterization of the PV modules, this system allows the measurement and recording of the current-voltage (*I-V*) curve data simultaneously with the module temperature, and all relevant meteorological parameters: irradiance, solar spectrum, environmental temperature, wind speed, humidity, etc., at adjustable time intervals. With the measurement of the *I-V* curve, the characteristic electrical parameters can be obtained which are: Short-circuit current ($I_{SC}$), open-circuit voltage ($V_{OC}$), maximum power ($P_M$), current ($I_{mp}$) and voltage ($V_{mp}$) at the maximum power point and the fill factor ($FF$), based on the procedures shown in (Fernández et al., 2018).

This paper presents the first results of the analysis of the generated power of different PV modules installed with respect to the cell temperature and irradiance, applying known methods and checking the scope of this measurement campaign to date. The paper is organized as follows: Section 2 describes the experimental setup, the instrumentation system, definitions of the parameters and the models used; Section 3 presents and discusses the first results of the experimental campaign; finally, in section 4 the conclusions are presented.

## 2. Materials and Methods

### 2.1. Measurement system

The home-made measurement system is installed on the roof of the Physics section (12° 4'S, 77° 4'W) in the PUCP (Fig. 1). All PV modules and instruments were placed at an angle of 20° facing north (to maximize the incident solar radiation) and were cleaned weekly to remove dust and dirt. The modules and sensor system are depicted in Fig. 1.

For the experimental campaign, three PV modules were studied: Standard poly-crystalline silicon (poly-Si) aluminum back surface field (Al-BSF) cells, mono-crystalline (c-Si) Heterojunction with Intrinsic Thin-Layer (HIT) cells, and amorphous and microcrystalline silicon (a-Si/µc-Si) thin-film tandem cells. Table 1 shows their main electrical parameters provided by the manufacturer.

The solar spectrum is recorded with an EKO MS-711 spectroradiometer (300-1100 nm), installed at the same angle as the PV panels. Note that an analysis of the recorded spectral distribution is out of the scope of this paper. However, in future studies, its impacts on the performance of different module technologies will be studied in detail.

**Fig. 1: Outdoor station for characterization of PV modules and the environmental sensors.**

**Tab. 1: PV Module electrical parameters under from the factory datasheet.**

| PV Module | $P_{max}$ (W) | $I_{SC}$ (A) | $V_{OC}$ (V) | $I_{mp}$ (A) | $V_{mp}$ (V) | $\gamma$ (%/°C) | $\alpha$ (%/°C) | $\beta$ (%/°C) | Efficiency (%) |
|---|---|---|---|---|---|---|---|---|---|
| Al-BSF | 270 | 9.32 | 37.9 | 8.75 | 30.8 | -0.41 | 0.05 | -0.31 | 16.5 |
| HIT | 330 | 6.07 | 69.7 | 5.70 | 58.0 | -0.26 | 0.06 | -0.24 | 19.7 |
| a-Si/µc-Si | 128 | 3.45 | 59.8 | 2.82 | 45.4 | -0.24 | 0.07 | -0.30 | 9.0 |

The measurements of the environmental variables are obtained by a Lufft WS500-UMB station. It can record air temperature, humidity, ambient pressure, air density, wind direction, and wind speed.

For the measurement of the irradiance, we have an EKO MS-80 pyranometer (0 – 4000 W/m$^2$) in a horizontal position and another at an angle of 20°. Also, we use a calibrated 5 W poly-Si PV module in short-circuit at an angle of 20° as a sensor of irradiance.

The complete diagram of the characterization system is shown in Fig. 2. This system can measure a total of up to fifteen individual PV panels periodically and consists of four main parts: the control system of the photovoltaic panels, the meteorological instruments, the capacitive load (as implemented Muñoz et al., 2011) and the control software developed in LabVIEW. The system is composed mostly of relays that are controlled by the digital output of an Arduino Mega 2560. These relays allow the passage of the sensors signal and the electrical energy of the PV modules. The module temperature was measured with two Class B PT100 sensors located on the back of each module, one at the center and other near the border.

The Control System of PV modules is composed of a multiplexer (MUX) of 16 channels and control boxes (B1-B15). Each box is connected to the positive and negative terminal and the PT100 temperature sensor of each PV module. Each channel of the multiplexer is connected to a different box. When a channel of the multiplexer is activated, the box is connected and allows the current passage of the PV module and their respective signal of the temperature sensors.

When a PV module is selected for measurement, the capacitive load is connected. First, to know the approximate charging time ($t_C$) of the capacitor (eq. 1), the irradiance and the temperature of the module are measured and stored to calculate the short-circuit current ($I_{SC}$) (eq. 2) and the voltage in open-circuit ($V_{OC}$) (eq. 3) values at that time from the characteristic parameters in STC.

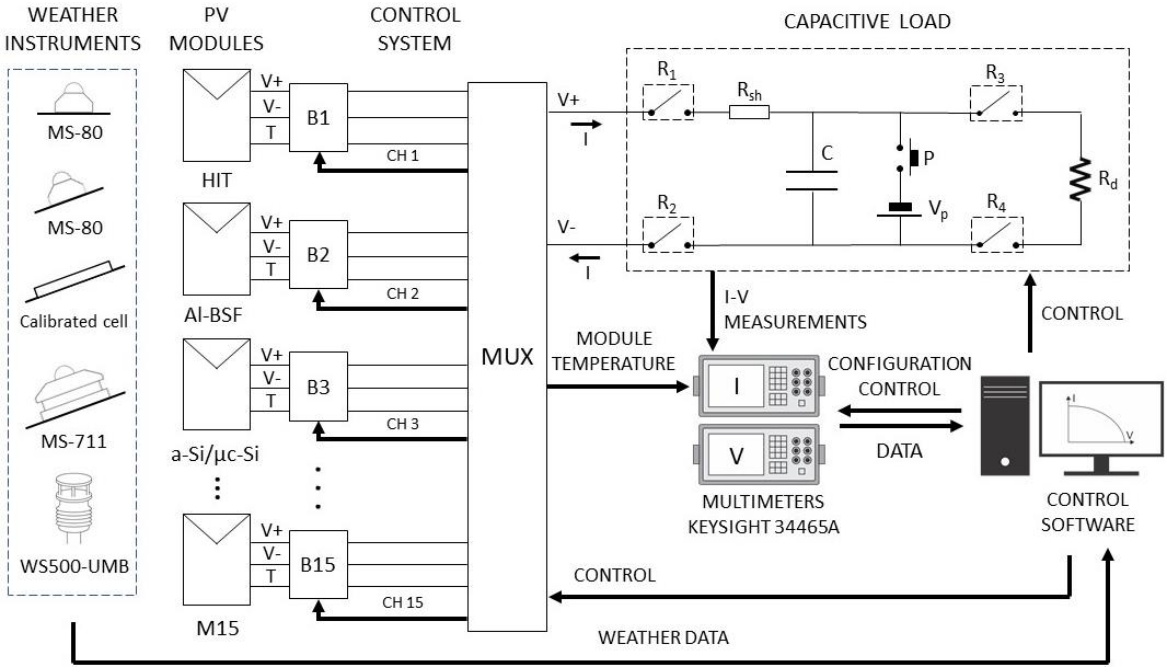


**Fig. 2: Diagram of the PV module characterization system.**

$$t_C = C\frac{V_{OC}}{I_{SC}} \quad \text{(eq. 1)}$$

$$I_{SC} = I_{SC}^{*}\frac{G}{G^{*}} \quad \text{(eq. 2)}$$

$$V_{OC} = V_{OC}^{*} - \beta(T_c - T_c^{*}) \quad \text{(eq. 3)}$$

Where $C$ is the capacitance value of the capacitor, $I_{SC}^{*}$ is the short-circuit current in STC, $G$ is the measured irradiance, $G^{*}$ is the irradiance in STC, $V_{OC}^{*}$ is the open-circuit voltage in STC, $\beta$ is the temperature coefficient of $V_{OC}$, $T_c$ is the cell temperature, and $T_c^{*}$ is the cell temperature in STC.

A more precise equation for $I_{SC}$ that includes temperature dependence is shown in eq. 4, where $\alpha$ is the temperature coefficient of the short-circuit current.

$$I_{SC} = I_{SC}^{*}\frac{G}{G^{*}}\left(1 + \alpha(T_c - T_c^{*})\right) \quad \text{(eq. 4)}$$

Once the capacitor charge time has been calculated, a negative preload voltage $V_p$ is applied to the capacitor by closing the switch $P$ for a short period to start the measurement in the second quadrant. Next, the relays $R_1$ and $R_2$ are closed to start the capacitor charge and synchronously record the current and voltage points with two Keysight 34465A multimeters respectively. Simultaneously, the solar spectrum and meteorological variables are also measured.

When the capacitor is charged, and the *I-V* points are stored, the relays $R_1$ and $R_2$ are opened. Finally, the relays $R_3$ and $R_4$ are closed, so that the resistor $R_d$ discharges the capacitor and a new measurement can be made. The Fig. 3 shows a screenshot of the program interface developed in LabVIEW.

A complete analysis of the uncertainty of the measurement using a similar instrumental configuration was published by (Montes-Romero et al., 2017). The same type of instruments were used as in this work, thus undermining the suitability and validity of the applied measurement system applied here.

When the process of design, construction, assembly, adjustment and verification of the complete system was completed, the experimental campaign of characterization of different commercial PV technologies in Lima began at the end of Abril 2019.

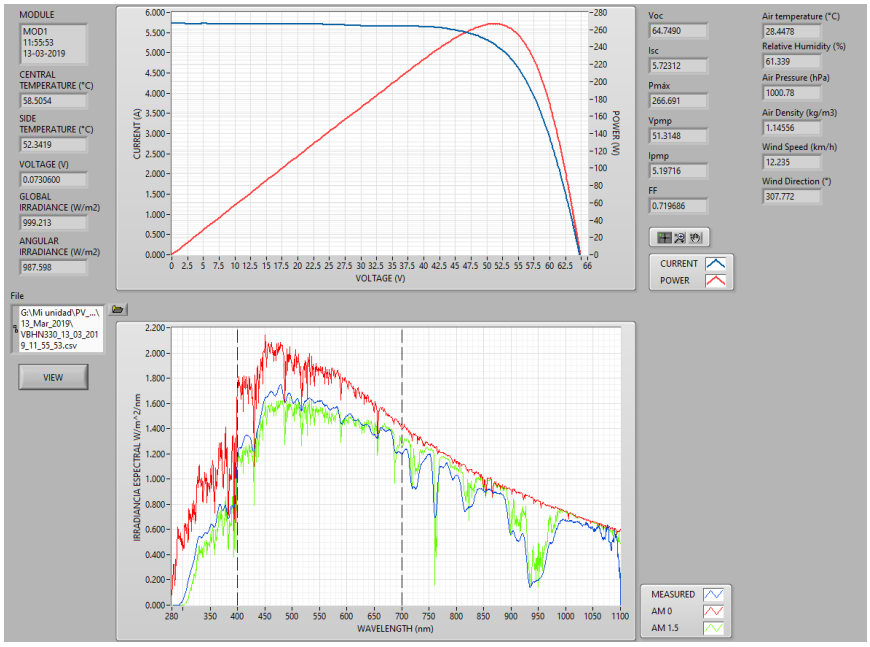


**Fig. 3: Screenshot of the LabView program developed for the control, measurement and analysis of data.**

### 2.2. Methodology

The objective of this research is to verify with what fidelity, simple analytical models can provide an estimate of the outdoor performance of different PV technologies in Lima. For this, two known methods to translate the maximum power under outdoor temperature and irradiance conditions to STC were used:

- Osterwald's method

This is one of the best known and simplest methods, as demonstrated in (Osterwald, 1986).

$$P_M = P_M^* \frac{G_i}{G_i^*}[1 - \gamma.(T_c - 25)] \quad \text{(eq. 5)}$$

Where $P_M^*$ is the maximum power in STC, $G_i$ is the incident irradiance, $G_i^*$ is the incident irradiance in STC, $\gamma$ is the temperature coefficient of $P_M$ and $T_c$ is the cell temperature.

- Constant Fill Factor (FFk) method

This method assumes that the fill factor remains constant in all operating conditions, also that the values of the short-circuit current and the open-circuit voltage vary linearly with the incident irradiance and the operating temperature, respectively, as presented in (Fuentes et al., 2007).

$$P_M = FF^* I_{SC} V_{OC} \quad \text{(eq. 6)}$$

Where $FF^*$ is the fill factor in STC (eq. 7), $I_{SC}$ is the short-circuit current (eq. 2) and $V_{OC}$ is the open-circuit voltage (eq. 3).

$$FF^* = \frac{P_M^*}{I_{SC}^* V_{OC}^*} \quad \text{(eq. 7)}$$

## 3. Results and discussion

More than 5000 *I-V* curves were recorded during the period of study along with the environmental variables (irradiance and temperature) and the solar spectrum for each module every 5 minutes. The data was collected on May, June, and July, when Lima is transitioning from autumn to winter seasons.

Fig. 4 shows the data distribution collected in percent with respect to different irradiance ranges for each PV technology. It is shown that for the months studied there is a large amount of data in low ranges of irradiance due to the respective seasons.

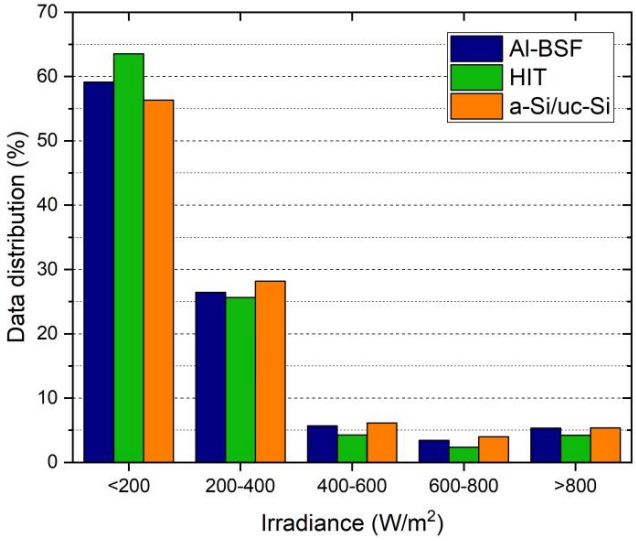


**Fig. 4:Data distribution collected for each PV technology.**

### 3.1. PV module characterization

First, the experimental characterization of the PV modules under study (Al-BSF, HIT and a-Si/µc-Si) was carried out. From the total of data collected, approximately 100 *I-V* curves were selected for each type of PV module, with the following criteria: to be acquired during the first days of the experiment (on clear days), at irradiations greater than 800 W/m$^2$ and in the central hours of the day. This allowed the losses associated with the angle of incidence and the spectral losses (Nofuentes et al., 2006) to be considered negligible.

For the characterization of the nominal power $P_M^*$ of the PV modules, eq. 8 was applied using the experimental values of the maximum power, irradiance, and temperature of the selected data:

$$P_M^* = \frac{G_i^*}{G_i} \frac{P_M}{[1 - \gamma.(T_c - 25)]} \quad \text{(eq. 8)}$$

Eq. 9, 10 and 11 were used to calculate the values of $I_{SC}$, $V_{OC}$ and the fill factor in STC.

$$I_{SC}^* = \frac{G_i^*}{G_i} \frac{I_{SC}}{[1 + \alpha(T_c - 25)]} \quad \text{(eq. 9)}$$

$$V_{OC}^* = V_{OC} + \beta(T_c - 25) \quad \text{(eq. 10)}$$

$$FF^* = \frac{P_M^*}{I_{SC}^* V_{OC}^*} \quad \text{(eq. 11)}$$

To analyze the reproducibility of the sample, statistical indices will be used: The average (eq. 12) was calculated for the values of $P_M^*$, $I_{SC}^*$, $V_{OC}^*$ and $FF$ for each PV technology. The results compared to the manufacturer's values with the relative difference are shown in Tab. 2. The standard deviation (eq. 13) and coefficient of variation (eq. 14) were calculated, which give information about the scattering of the data.

$$\bar{x} = \frac{\sum X(i)}{N} \quad \text{(eq. 12)}$$

$$\sigma_I = \sqrt{\frac{\sum (X(i) - \bar{X})^2}{N}} \quad \text{(eq. 13)}$$

$$CV(\%) = \frac{\sigma_I}{\bar{X}} \times 100 \quad \text{(eq. 14)}$$

**Tab. 2: Characteristic values in STC of the PV modules calculated from the experimental irradiance and cell temperature data, and compared with respect to the values given by the manufacturer.**

| | | Experimental Value | Standard deviation | Coefficient of variation | Manufacturer information | Relative difference |
|---|---|---|---|---|---|---|
| **Al-BSF** | $P_M^*$ **(W)** | 269.2 | 1.87 | 0.7% | 270 | 0.3% |
| | $I_{SC}^*$ **(A)** | 9.45 | 0.13 | 1.4% | 9.32 | -1.4% |
| | $V_{OC}^*$ **(V)** | 37.2 | 0.15 | 0.4% | 37.9 | 1.8% |
| | $FF^*$ | 0.77 | 0.008 | 1.0% | 0.76 | -0.1% |
| **HIT** | $P_M^*$ **(W)** | 324.6 | 5.90 | 1.8% | 330 | 1.6% |
| | $I_{SC}^*$ **(A)** | 6.05 | 0.13 | 2.1% | 6.07 | 0.3% |
| | $V_{OC}^*$ **(V)** | 70.4 | 0.49 | 0.7% | 69.7 | -0.9% |
| | $FF^*$ | 0.76 | 0.010 | 1.3% | 0.78 | 2.2% |
| **a-Si/µc-Si** | $P_M^*$ **(W)** | 127.9 | 2.08 | 1.6% | 128 | 0.1% |
| | $I_{SC}^*$ **(A)** | 3.32 | 0.07 | 2.0% | 3.45 | 3.8% |
| | $V_{OC}^*$ **(V)** | 59.1 | 0.17 | 0.3% | 59.8 | 1.1% |
| | $FF^*$ | 0.65 | 0.004 | 0.6% | 0.62 | -5.1% |

In Table 2, low standard deviation values indicate that most data are close to the mean and low coefficient of variation values indicate that there is little dispersion and variability in the data.

### 3.2. Analytical models vs experimental measurements

With the prior experimentally characterized value of $P_M^*$ and the experimental irradiance and temperature data, the power is calculated with the Osterwald (eq. 5) and FFk models (eq. 6-7).

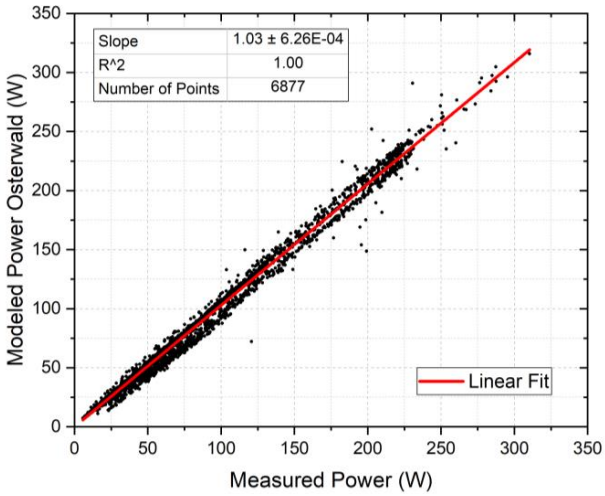


**Fig. 5. Modeled power values ($P_M$) calculated through Osterwald model vs the measured for the Al-BSF PV module.**

Fig. 5 exemplary shows the graph of the power modeled by Osterwald vs the power measured for the Al-BSF technology. As can be seen in the slope value of the linear correlation and the determination coefficient ($R^2$) close or equal to 1, respectively, the applied Osterwald model can reasonably estimate the measured power value. However, the value of the slope is slightly greater than 1 indicating that the Osterwald model is slightly overestimating the value of the modeled power. We suggest that this is most likely due to an overestimated nominal power $P_M^*$ of the modules. Therefore, we propose to introduce a correction factor ($\kappa$) for further analysis.

$$P_M^{*,corr} = \kappa \times P_M^* \qquad \text{(eq. 15)}$$

Tab. 3 shows the calculated correction factors for each model applied to each technology, values less than 1 indicate that the modeled values are being overestimated and values greater than 1 indicate that the modeled values are being underestimated. An over- or under estimation implies that in addition to irradiance and module temperature other factors need to be taken into account for modeling the power, such as spectral distribution and/or direct and diffuse irradiance components.

**Tab. 3: Correction factor ($\kappa$) values for the Osterwald and FFk models applied to the $P_M^*$ and $FF^*$ respectively.**

| | Model | Experimental value | Correction factor ($\kappa$) | Corrected modeled value |
|---|---|---|---|---|
| **Al-BSF** | $P_M^*$ (W), (Osterwald) | 269.24 | 0.97 | 261.17 |
| | $FF^*$, (FFk) | 0.77 | 0.96 | 0.73 |
| **HIT** | $P_M^*$ (W), (Osterwald) | 324.60 | 0.97 | 314.86 |
| | $FF^*$, (FFk) | 0.76 | 0.97 | 0.74 |
| **a-Si/µc-Si** | $P_M^*$ (W), (Osterwald) | 127.93 | 1.01 | 129.21 |
| | $FF^*$, (FFk) | 0.65 | 1.02 | 0.66 |

The values of the modeled $P_M$ calculated using the correction factor vs the experimentally measured power are shown in Fig. 5, 6 and 7 for each PV technology.

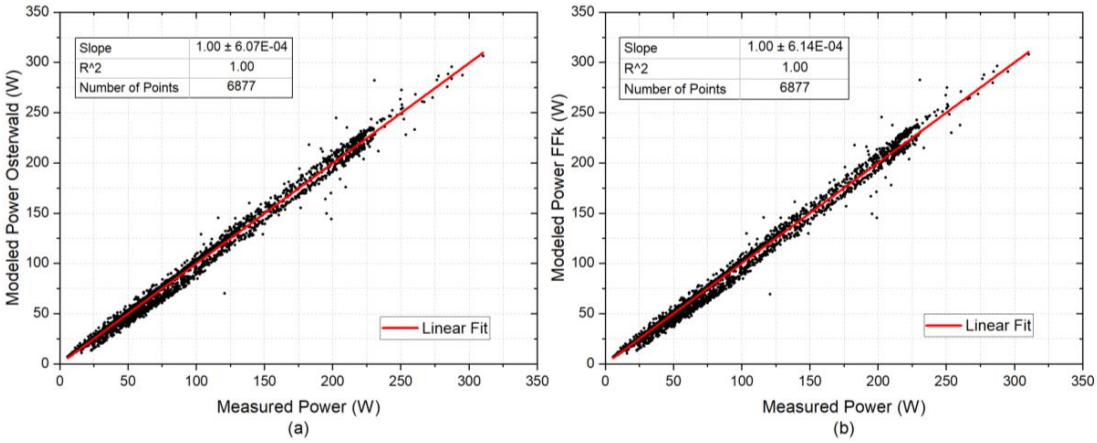


**Fig. 6: Modeled power calculated using $P_M^{*,corr}$ through (a) Osterwald and (b) FFk models vs the measured for the Al-BSF PV module.**

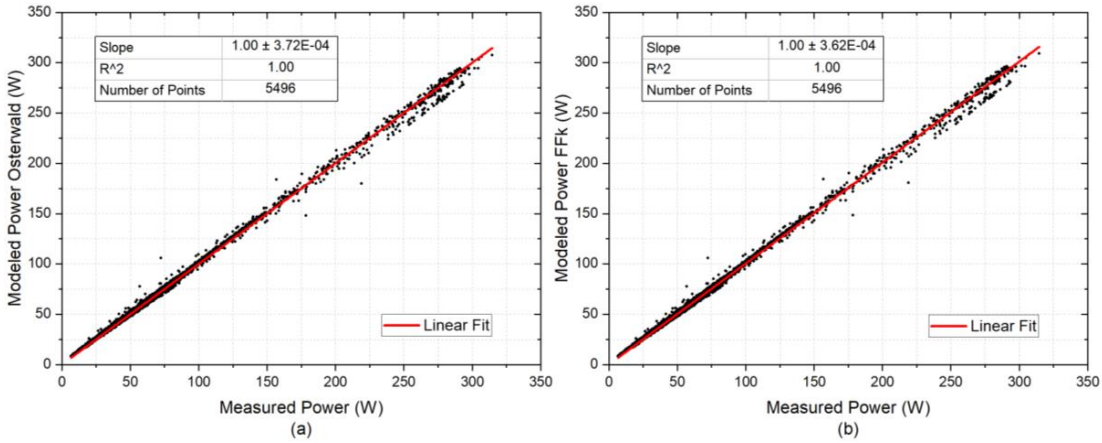


**Fig. 7: Modeled power calculated using $P_M^{*,corr}$ through (a) Osterwald and (b) FFk models vs the measured for the HIT PV module.**

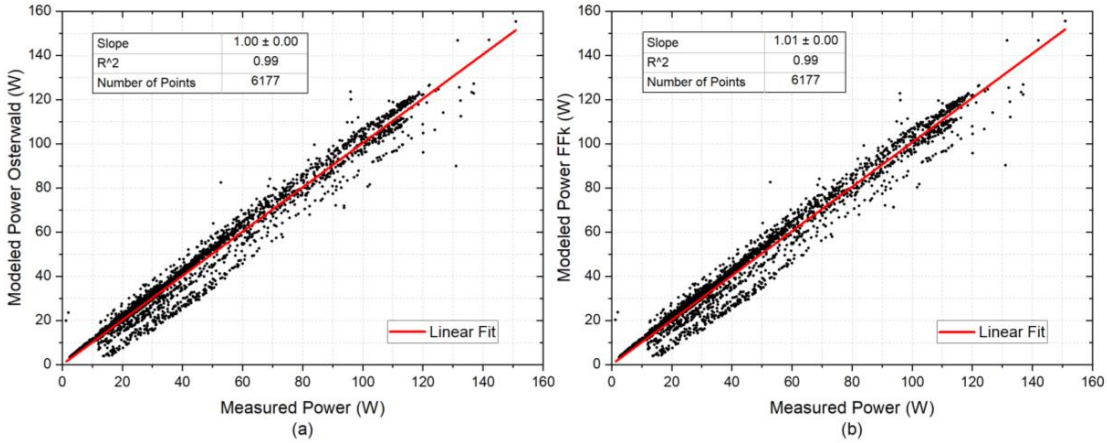


**Fig. 8: Modeled power calculated using $P_M^{*,corr}$ through (a) Osterwald and (b) FFk models vs the measured for the a-Si/µc-Si PV module.**

To evaluate the goodness of each model after applying the correction factor, the statistical parameters *root means square error* (RMSE) and *mean bias error* (MBE) were calculated. The RMSE (eq. 16) provides information on the scattering of the modeled power values vs the measured ones, while the MBE (eq. 17) provides the average deviation of the modeled power values from the measured ones.

$$RMSE(\%) = 100\sqrt{\frac{\sum_{i=1}^{N}(P_{Ti} - P_{Oi})^2}{N}} \Big/ \left(\frac{1}{N}\sum_{i=1}^{N} P_{Oi}\right) \quad \text{(eq. 16)}$$

$$MBE(\%) = 100\frac{\sum_{i=1}^{N}(P_{Ti} - P_{Oi})}{N} \Big/ \left(\frac{1}{N}\sum_{i=1}^{N} P_{Oi}\right) \quad \text{(eq. 17)}$$

Where $P_{Ti}$ is the $ith$ modelled value of the power after applying the correction factor, $P_{Oi}$ is the $ith$ measured value of the power and $N$ is the number of modelled or measured values.

Fig. 9 (a) shows the RMSE values for the different PV technologies after applying the Osterwald and the FFk model. On the one hand, it shows that the HIT module is the PV technology with a lowest RMSE and, thus, dispersion. This may indicate that this PV technology is less susceptible to environmental conditions not considered by the models and that may be dominant in Lima between the autumn and winter months. On the other hand, the a-Si/µc-Si module is the technology with the highest RMSE and, thus, dispersion. This is in accordance with results presented in (Torres-Ramírez et al., 2014), probably these technologies based on thin-films and tandems are more dependent on external effects that are not considered in these models such as the spectral effect (Hirata et al., 1995).

Fig. 9 (b) shows the MBE values for the different applied PV technologies and models. The values less than 1% mostly for the Osterwald model and the FFk in the different PV technologies indicate that the models interpret the measurement system very well, with a lower error for Al-BSF and a higher error for a-Si/µc-Si.

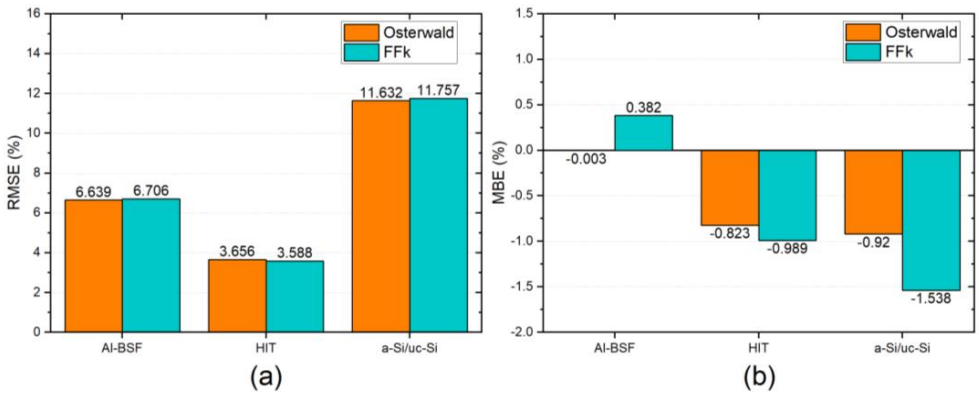


**Fig. 9: (a) RMSE and (b) MBE values for the different PV technologies after applying the Osterwald method and the FFk method.**

## 4. Conclusions

For the appropriate development and implementations of PV technologies in a country, it is necessary to conduct a detailed study of the different commercial versions of these technologies. For this, it is essential to have research laboratories that allow the study and analysis locally.

The PUCP, in collaboration with the University of Jaén-Spain, using own funds and those of the Peruvian government, in the framework of the project "Caracterización, modelado y estudio del comportamiento de diferentes generaciones de tecnologías fotovoltaicas frente a las condiciones climáticas del Perú" (Characterization, modelling and study of the behavior of different generations of photovoltaic technologies with respect of Peru's climatic conditions), is making the first advances so that Peru has a laboratory for the analysis and calibration of PV modules under outdoor working conditions. This laboratory is the first in the country that has the appropriate instrumentation to perform calibration processes and certification of PV modules that could be offered to companies or public institutions, as well as detailed research studies of the behavior and degradation of different commercial PV technologies depending on the particular operating climate conditions of the city of Lima (irradiance levels, operating temperature, humidity, spectral distribution, etc.).

After a year of design, construction, assembly and calibration, it can be affirmed that the PV module characterization laboratory, based on the complete tracing of its characteristic *I-V* curve, has been fully

operational since the end of April of 2019. In this work some first advances of the investigations carried out to date have been presented. As a previous step to carry out any analysis of PV technologies, an experimental calibration process of the fundamental electrical parameters of the PV modules under study has been carried out. This experiment allowed us to affirm that the experimental outdoor results reasonably comply with the indoor-data of electrical parameters provided by the module manufacturers.

Subsequently, and during the following three months, an experimental study has been carried out to investigate the applicability and validity of the two analytical models: Osterwald and Constant Fill Factor methods. These two represent the simplest and most commonly used methods by the scientific community to interpret such experimental results for PV technologies. Furthermore, each method has been discussed in terms of their goodness of the power prognosis they offer when compared with the experimental measurements. It should be emphasized that the three months of study, together with August, are the most unfavorable for the operation of PV technology in this geographical area, due to the peculiarities of Lima's climate during winter months.

Typically, at least one or two years of the experimental campaign are necessary to publish definitive conclusions on outdoor PV experiments. Nevertheless, even with only three months of data presented in this work, the partial conclusions obtained to date are of upmost interest for the local community.

The experimental characteristic curves of the three PV technologies were acquired under conditions of irradiance and temperature representative of Lima's climate during the months of study. When comparing the modeled powers with the experimental measures, the good indexes of linear correlation ($\approx 1$) and of coefficient of determination ($R^2 > 0{,}98$) indicate a very good prediction reliability of the models.

Furthermore, the applied corrections factors > 1 for the a-Si/µc-Si indicate that the applied models may underestimate the nominal power of the tandem technology under the local climate conditions. Whereas a correction factor of < 1 indicates that the nominal power of the Al-BSF and HIT modules may be overestimated for the same conditions. This hypothesis is in accordance with the conclusions shown in previous studies (Romero-Fiances et al., 2018) where performance ratios close to 1 demonstrate a proper functioning of the a-Si/µc-Si technology on PV-system level under the climate of Lima. However, longer and more profound studies need to be performed to explore this hypothesis. For instance, more complex theoretical models will have to be evaluated that consider particularly the spectral distribution (Nofuentes et al., 2013) as well as the direct and diffuse components of the irradiance. This will be subject to the broader experimental campaign currently in process to deepen the knowledge of the behavior of the different PV technologies in Lima, Peru.

## 5. Acknowledgments

The authors are grateful to the researchers of the IDEA research group from the UJA and of the MatER research group from the PUCP for their support and advice. This work was partially funded by the National Council of Science, Technology and Technological Innovation (CONCYTEC) under the PhD scholarship program (236-2015-FONDECYT). Additional support has been provided by the Peruvian National Fund for Scientific and Technological Development (FONDECYT) through Contract N°124-2018-FONDECYT. We are grateful for the support given by the Andalusian International Cooperation Agency–AACID through the project “Emerging with the Sun. Institutional support to the CER-UNI in the field of electricity generation using photovoltaic technology” (Project Nº 2012DEC206). Finally, we acknowledge the support provided by the Vicerectory of the PUCP through research activity PO0088 and grant no. 2019-3-0041.

## 6. References

Fuentes, M., Nofuentes, G., Aguilera, J., Talavera, D. L., Castro, M., 2007. Application and validation of algebraic methods to predict the behaviour of crystalline silicon PV modules in Mediterranean climates. Solar Energy, 81(11), pp. 1396-1408.

Hirata, Y., Tani, T., 1995. Output variation of photovoltaic modules with environmental factors-I. The effect of spectral solar radiation on photovoltaic module output. Solar Energy, 55(6), pp. 463-468.

Kottek, M., Grieser, J., Beck, C., Rudolf, B., Rubel, F., 2006. World map of the Köppen-Geiger climate classification updated. Meteorologische Zeitschrift, 15(3), pp. 259-263.

Montes-Romero, J., Piliougine, M., Muñoz, J., Fernández, E., De la Casa, J., 2017. Photovoltaic device performance evaluation using an open-hardware system and standard calibrated laboratory instruments. Energies, 10(11), p. 1869.

Muñoz, J. V., De la Casa, J., Fuentes, M., Aguilera, J., Bertolín, J. C., 2011. New portable capacitive load able to measure PV modules, PV strings and large PV generators. 26th European Photovoltaic Solar Energy Conference and Exhibition, Vol. 1, pp. 4276-4280.

Nofuentes, G., Aguilera, J., Santiago, R. L., De La Casa, J., & Hontoria, L., 2006. A reference-module-based procedure for outdoor estimation of crystalline silicon PV module peak power. Progress in Photovoltaics: Research and Applications, 14(1), pp. 77-87.

Nofuentes, G., De la Casa, J., Torres-Ramírez, M., Alonso-Abella, M., 2013. Solar spectral and module temperature influence on the outdoor performance of thin film PV modules deployed on a sunny inland site. International Journal of Photoenergy, 2013.

Osterwald, C. R., 1986. Translation of device performance measurements to reference conditions. Solar cells, 18(3-4), pp. 269-279.

Romero-Fiances, I., Muñoz-Cerón, E., Espinoza-Paredes, R., Nofuentes, G., De la Casa, J., 2019. Analysis of the Performance of Various PV Module Technologies in Peru. Energies, 12(1), p. 186.

Torres-Ramírez, M., Nofuentes, G., Silva, J. P., Silvestre, S., Muñoz, J. V., 2014. Study on analytical modelling approaches to the performance of thin film PV modules in sunny inland climates. Energy, 73, pp. 731-740.

## 7. Web References

[1] https://www.inei.gob.pe/prensa/noticias/poblacion-del-peru-totalizo-31-millones-237-mil-385-personas-al-2017-10817/ (accessed on 10 July 2019)

[2] https://www.gob.pe/institucion/minem/noticias/19687-peru-es-nombrado-vicepresidente-de-la-alianza-solar-internacional-por-la-region-latinoamerica-y-caribe (accessed on 10 July 2019)

[3] http://www.minem.gob.pe/_detallenoticia.php?idSector=8&idTitular=8660 (accessed on 17 July 2019)

[4] http://www.minem.gob.pe/_detallenoticia.php?idSector=6&idTitular=9159 (accessed on 17 July 2019)